Critical behavior of a strain percolation model for metals

Y. Shim,[1,2] L. E. Levine,[2] and R. Thomson[2]
[1]*Center for Simulational Physics, University of Georgia, Athens, Georgia 30602*
[2]*Materials Science and Engineering Laboratory, National Institute of Standards and Technology, Gaithersburg, Maryland 20899*
(Received 8 May 2001; published 11 April 2002)

Extensive simulations of a strain percolation model for a deforming metal have been performed to examine its strain behavior. We find that the total strain exhibits critical power-law behavior that is well explained by two-dimensional percolation theory. Near the critical point, most of the strained cells organize themselves around a state having the minimum or at least marginally stable strain regardless of the initial conditions. A strain much greater than the minimum stable strain generally decays to a lower value when transmitted to an unstrained cell. The universal behavior of the total strain in the system is a consequence of the self-organizing character of the strain in the critical cluster. Although the probability distributions for the total strain and cluster size appear to exhibit nonuniversal behavior, this may merely represent a transient response before crossover to a true asymptotic, universal behavior occurs. Other critical aspects of the model are also discussed.

DOI: 10.1103/PhysRevE.65.046146 PACS number(s): 62.20.Fe, 64.60.Ak, 81.40.Ef

I. INTRODUCTION

In previous papers, we introduced and reported on the geometrical aspects of a percolation model for strain in metals [1,2]. We believe this model corresponds, in stage III metal deformation, to the fine slip line structure formed in all stages of metal deformation. See Refs [3,4] for current reviews of the general subject. In stage I, the slip is composed exclusively of such lines, which can be as long as the specimen side, are parallel to the primary slip planes, are distributed quite uniformly on the surface, and have a height of the order of a few Burgers vectors [5,6]. As deformation proceeds, secondary slip begins, the fine slip becomes more heterogeneous, and by stage III, has localized into gross slip bands [5,6]. But within these bands, the fine slip is still present as a well defined fine structure [7,8], with an apparent minimum distance between the slip lines of the order of 50 nm, and a height still of the order of a few Burgers vectors [8]. In addition to the strong localization of the fine slip into bands, the slip is highly localized in time, appearing as bursts of strain, or avalanches, lasting less than 0.1 s [9] (and perhaps much less than that [10]) and separated by much longer times. Pond measured relaxation times between bursts of the order of 2 s [9], but the time between bursts is almost certainly strain rate dependent. It is not clear whether only one, or perhaps a few slip line production events are produced in each strain burst [9].

We believe the production of these fine slip lines, which are the elementary events underlying the entire deformation process, can be modeled in stage III by the strain percolation model [1,2]. (The model assumes the presence of a well formed and partially ordered dislocation cellular structure, which is only formed during and after stage II, when extensive secondary slip makes its appearance.) In previous papers, we have developed an approximate mean field description of the model, studied the purely geometrical aspects of the strain clusters generated in the model, and shown that these geometrical aspects are in the same universality class as standard percolation theory [11]. But it is the strain generated by the system that is essential to the physical problem. Therefore, our study of the model has been incomplete, because the main object of study in the previous papers was the geometrical aspects of the strain clusters, not the associated strain. In the current paper, by focusing directly on the strain variable, itself, which has no counterpart in standard percolation theory, we will make predictions for fine slip strain that can then be subjected to experimental verification.

In particular, such experimental explorations are currently in progress using atomic force microscopy to study the slip line height profiles and transmission electron microscopy to study the underlying dislocation cell structure. Additional collaborative work is planned to use acoustic emission and photoemission experiments to study the time dependence of the percolation events. So the results of this paper will stimulate extensive experimental efforts that can be used both to verify the basic model and show how the model should be modified and extended. In contrast to the strain predictions, the purely geometrical aspects of the model are not so easily accessible to experimental measurement.

Our percolation model for strain has been motivated by a conviction that statistical aspects of metal deformation are dominant, and that the concepts of percolation apply very naturally to the generation of strained clusters during metal deformation. Indeed, percolation can be found in many fields of physics, e.g., fracture networks [12], electrical conductivity [11], flow in a random media [13], etc. A common feature of the systems is critical power-law behavior characterized by a few critical exponents and their fractal structures near the critical point. A self-organized critical (SOC) system [14–17] exhibits such features without the need to fine-tune parameters. Using a simple cellular automaton sandpile model, Bak *et al.* showed that the system evolves into a barely stable critical state at which a scale-invariant fractal structure emerges due to the lack of length (time or size) scales present in the system [14]. A characteristic feature in SOC systems is a power-law decay in the size distribution of the dissipation events. A deforming material has been shown to exhibit such a feature in that an increase of the plastic strain results in avalanches that occur within a very short time scale.

 ©2002 The American Physical Society

It is well known that a deforming metal is a highly disordered, complex system on various length scales because, during the deformation process, a large number of dislocations (line defects) are produced and they interact with each other by long-range $1/r$ forces as well as short-range forces. Due to the increase in dislocation density and the complex mutual interactions between dislocations during plastic deformation, work hardening occurs. As a result of the deformation process, heterogeneous cell structures are formed, in which high dislocation density walls surround regions of very low dislocation density; see Ref. [3] for a critical review of dislocation patterning. Therefore, a theory of work hardening must explain both the cell formation process and the transport of mobile dislocations through the walls of the cell structure. In spite of intensive efforts extending over several decades, a solution to the problem of work hardening remains elusive.

Despite all the complexity occurring during the deformation, a fractal structure has been identified in transmission electron micrographs of the dislocation cell structure of a Cu single crystal after tensile deformation [18] and in a simulation of a stochastic dislocation dynamics model [19]. A box-counting analysis (fractal analysis) of the structures reveals that the cell size and dislocation wall size distributions exhibit power-law behavior [19,20]. Another interesting feature given in Ref. [20] is a shape change in the probability distribution of the total dislocation densities, which is the steady-state solution of a theoretical two-dimensional dislocation density evolution equation proposed for the transmission electron micrograph. Depending on the noise intensity in the system that is inversely proportional to the external stress, the distribution changes from a power-law decay to an asymmetric bell shape function as the external stress increases. From the statistical physics point of view, these critical properties of a deforming metal confirm that the system should be treated as a stochastic dynamical system.

Kocks [21] proposed a statistical model of a dislocation line gliding through random immobile obstacles under an external stress, and the resulting critical shape of the dislocation line [22] is quite similar to that observed in an invasion percolation model in random media [13]. In the Kocks model, the externally applied stress must be larger than the yield stress in order for the dislocations to percolate through the obstacle distribution; this leads to the existence of a critical stress at the depinning transition point. Since a dislocation line in the model is driven through the random immobile obstacles by an external stress, we note that the physical picture of the motion is rather similar to that of a driven interface or line motion in a quenched random noise by an external force [23]. But the Kocks model focuses on the percolation of a single dislocation through a set of obstacles, whereas ours addresses the statistical transport of collective groups of dislocations through the 3D cell structure. Thus, the Kocks model applies to the early stages of deformation near the initial yield, whereas ours applies to a system near stage III after significant strain has occurred, and dislocation ordering is well advanced.

In this paper, we determine the universality class of the strain related quantities of the strain percolation model and study strain-strain correlation functions in the light of the geometrical aspects of the model. It is also important to stress that although our model is a simplified statistical model of a deforming metal, we hope to capture the key mechanisms of strain propagation and to explain statistical properties of the system in terms of the universality class. This paper is organized as follows. In Sec. II, we present our strain percolation model in detail and simulation results are given in Sec. III. We conclude in Sec. IV.

II. MODEL

First, we assume that a dislocation cell structure exists in a metal single crystal and then, as a response to an external stress increment $\delta\sigma_{\mathrm{ext}}$, a strain s_0, is nucleated at some weak cell on a slip plane. We consider two different mechanisms of strain propagation from a strained cell to unstrained neighboring cells. In the first case (case I), a relatively stable wall can act as a source of new dislocations and the strain s propagates by activating sources in such walls. Since s is equivalent to a small pileup of dislocations expanding in the strained cell, the stress acting on the wall barrier between the two cells is proportional to the number of dislocations in the pileup [24]. In this case, we then assume that the magnitude of strain induced in an unstrained cell is linearly proportional to the strain in a neighboring strained cell. The proportionality factor is a stochastic variable that reflects the distribution of sources within the walls. In the second case (case II), as an additional relatively rare mechanism, unstable locks within a wall can be unzipped by a nearby dislocation pileup that can lead to a large localized strain with the amount of strain P_2. Since the probability K of unzipping a lock is assumed to be linearly proportional to the number of dislocations in the pileup, $K=sK_0/P_2 \ll 1$. K_0 is a proportionality constant. In case I, $K_0=0$.

The law of strain propagation from a strained cell to a neighboring unstrained cell is thus given as

$$s^*=\begin{cases} P_2 & \text{for } 0 \leqslant \eta_1 \leqslant K \\ sP_1\eta_2 & \text{for } K < \eta_1 \leqslant 1, \end{cases} \tag{1}$$

where s^* is the number of dislocations induced in the previously unstrained cell and s is the number in its strained neighbor. P_1 is a measure of how efficiently the cell walls can transmit strain from a strained cell to an unstrained one via source activation. η_1 and η_2 are random numbers with $0 \leqslant \eta_1,\ \eta_2 \leqslant 1$. The values of these parameters must be determined either from experiment or from dislocation simulations (i.e., from the underlying cell physics).

When an unstrained cell has more than one strained neighbor, there are several possible rules that can be used for determining the transmitted strain. In this paper, we consider two different sets of rules, referred to as models *A* and *B*. In model *A*, the amount of strain transmitted to the unstrained cell s^* takes the largest value among the contributions from its neighbors. In model *B*, the unstrained cell takes the first successful strain transmission as the computer program steps through the strained neighbors. In both models, growth of a strained cluster takes place only on its periphery. Since dislocations are discrete entities, the minimum amount of strain

that can be induced in an unstrained cell is unity; if $s^*<1$ in a simulation, we set $s^*=0$. In a real metal, the maximum amount of strain that can be induced in a cell, s_m, depends on the dislocation wall properties. Accordingly, if $s^*>s_m$, then s^* is set to s_m. We consider s_m to be a model parameter. Thus, the independent model parameters are P_1, P_2, K_0, s_0, and s_m.

We note that a great deal of information on the values of these parameters, as well as the functional form for the stochastic function, can be obtained by atomic force microscopy measurements of slip lines. For example, measurements looking at the variation of slip line height *along* individual slip lines could yield information on the distribution of strains occurring within a percolating cluster. This information would need to be combined with transmission electron microscopy data on the underlying dislocation cell structures. *In situ* high-resolution reflection x-ray topography could also provide useful information by simultaneously imaging both the formation of slip lines and the underlying near-surface dislocation structures.

Our simulations have been carried out on a 2D regular square lattice, with no cell size variation, where the linear system size is L, and all the length scales in the system are measured in units of a linear cell size $r_c=1$. All of the strain variables are measured in units of the minimum amount of strain that can be induced in an unstrained cell, i.e., $s_{min}=1$. As noted in the Introduction, in a standard percolation problem, a change in the lattice geometry changes the percolation threshold but does not change the universality class. A single cluster is grown from the center of the system until growth stops. 2D is the relevant dimension for this problem since we consider slip on only a single slip plane. Although this growth algorithm is similar to that of Leath [25], it is a correlated percolation problem unlike other random percolation problems since the probability that a site is strained depends on the strain of its neighbors as given in Eq. (1). Most of the reported simulations focus on model *A* for both subcritical and supercritical regimes but relevant results for model *B* are given in Sec. III *C*. We first show results for the subcritical regime for model *A*.

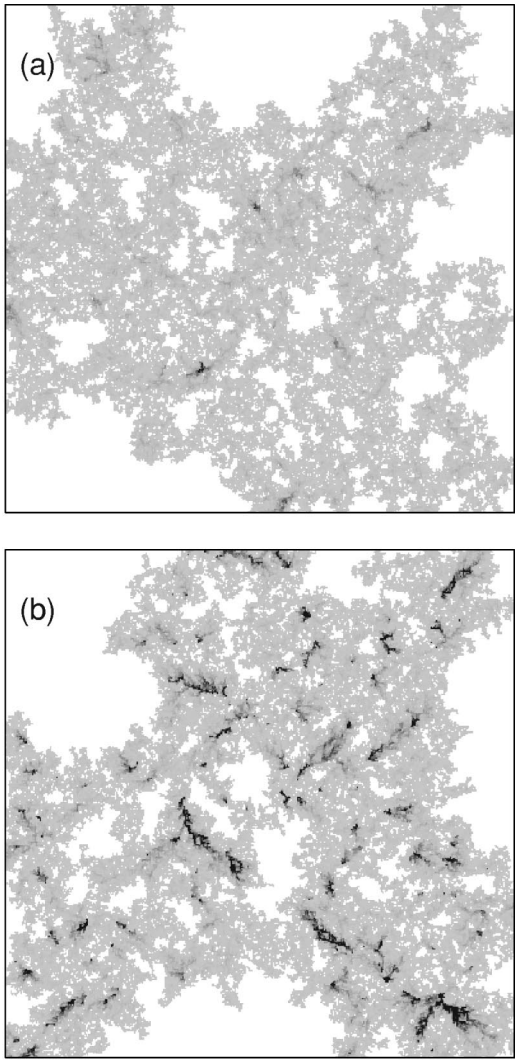

FIG. 1. Spanning cluster at the critical point. Darker color represents larger strain and lighter color represents smaller strain in a cell. Here, $s_0=2.2$ and $L=401$. (a) is for $K_0=0$ with $P_1=1.306$ and $s_m=\infty$, and (b) is for $K_0=0.01$ with $P_1=1.2926$, $P_2=40$, and $s_m=40$. Note that (a) is for case I and (b) is for case II.

III. RESULTS

A. Subcritical regime ($P_1<P_{1c}$)

The general shape of a spanning cluster at the critical point is fractal, as shown in Fig. 1. The overall fractal shape does not depend on the detailed model parameters as long as the system is near the critical point. On the other hand, the distribution of strain changes dramatically when the density of the unstable locks becomes nonzero. When $K=0$ (case I), the spanning cluster shown in Fig. 1(a) for a small initial strain $s_0=2.2$ is quite ramified, but the localized regions having a large strain are relatively compact. For this set of parameters, the critical point is at $P_{1c}=1.306(2)$ as shown in Fig. 2. For a large s_0, the system has a large strain near the initiation point, but this strain decays quickly as the cluster extends. For $s_0=10$ and $K_0=0$, we obtained $P_{1c}=1.3064(4)$.

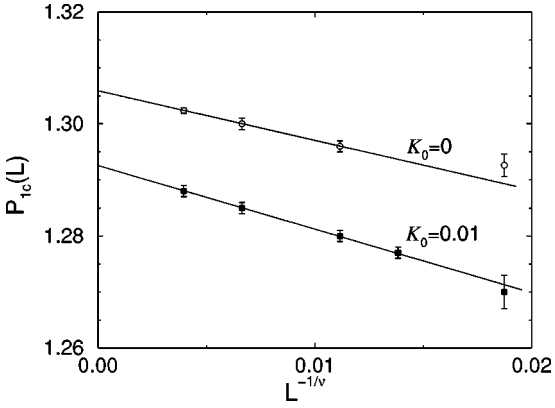

FIG. 2. The percolation threshold for cases shown in Fig. 1. $P_{1c}=1.306(2)$ for Fig. 1(a) and $P_{1c}=1.2926(30)$ for Fig. 1(b).

When $K \neq 0$ (case II), some of strained cells develop a large strain mainly due to the unzipping process, which, in turn, increases the probability of activating the unzipping process ($K = sK_0/P_2$) in a neighboring cell. This leads to ridge shaped regions of large strain as shown in Fig. 1(b). Note that if such a process does not occur consecutively in a nearby cell, the large strain decays rapidly. Furthermore, when the unzipping process is activated, the critical value for P_1 becomes lower than that for case I because the system has a greater chance of developing a large strain. Figure 2 shows the extrapolation of the critical point (percolation threshold) to the thermodynamic limit ($L \to \infty$) for the cases shown in Figs. 1(a) and 1(b). Not surprisingly, the critical value for P_1 is insensitive to changes in s_0 and s_m, but for case II, this critical value is quite sensitive to changes in P_2 and K_0.

We found previously [2] that for case I the mean strain defined as the strain per strained cell is $\langle s \rangle_c \approx 2$ at the critical point. Insight into the mechanism responsible for this mean strain can be obtained by considering how strain propagates just below and at the critical point. Just below the critical point, the average strain on the periphery of a growing cluster must decrease until the growth stops. At the critical point, the strain propagation stabilizes to a small but finite value that is close to the minimum stable value of strain. For any trial transmission, on the average, the value of the strain in the strained site must be such that from Eq. (1),

$$P_{1c} \langle \eta_2 \rangle \langle s \rangle \geq 1. \tag{2}$$

Thus, the minimum stable value of strain is given approximately by $\langle s \rangle_{stable} \approx 2/P_{1c} \approx 1.5$, which, as expected, is slightly smaller than the measured mean strain. For case II, the mean strain at the critical point becomes larger since the large strains from the unzipping events give an additional strain increment.

From the argument just presented, the existence of a critical mean strain is seen to depend directly on the requirement of a minimum value for the transmitted strain, and thus on the discrete nature of the dislocations. Not surprisingly, the mean strain will be seen to play an important physical and mathematical role in the following.

A useful measure of how strain is apportioned among the cells is given by the strain probability distribution function, $\mathcal{P}(s)$, where $\mathcal{P}(s)\,ds$ is the average number of sites in a simulation having the strain s. As can be seen in Fig. 3, $\mathcal{P}(s)$ is a slowly varying function near the minimum strain. For larger strains, however, the strain distribution exhibits a fast power-law decay with $\mathcal{P}(s) \sim s^{-4.41}$ when $K_0 = 0$, but when $K_0 \neq 0$, it deviates from the power law. The difference between the two curves for $s_0 = 2.2$ and 10 is due to finite-size effects, since for an infinite system, the behavior near the origin where the strain initiates will have negligible influence on the total system behavior. As predicted above, $\langle s \rangle_{stable}$ is very close to 1.5. A strain $s > \langle s \rangle_{stable}$ is most likely to decay to a lower value when transmitted to an unstrained cell. Since Figs. 1(a) and 1(b) use the same gray scale and the lightest gray is roughly $\langle s \rangle_c$, most of the cells seem to be near the minimum or at least marginally stable state regardless of the initial conditions, a behavior similar to that found in other SOC systems.

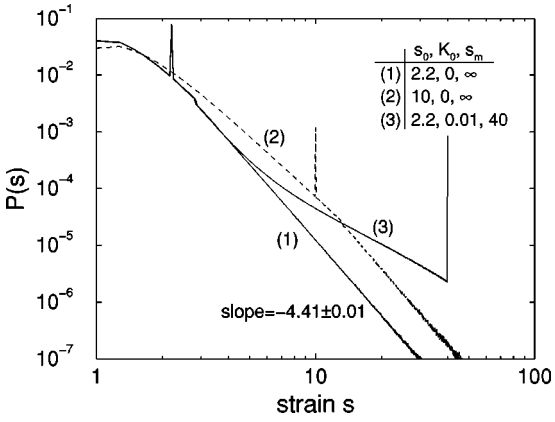

FIG. 3. Probability distribution of having strain s at the critical point for the cases shown in Fig. 1 and also for a larger initial strain of $s_0 = 10$ with $K_0 = 0$. Sharp peaks are due to the initial strain (s_0) and the result of the unzipping process ($P_2 = 40$).

Figure 4 shows the critical behavior of the total strain T defined as $T(P_1) = \langle \Sigma_{\mathbf{r}} s(\mathbf{r}, P_1) \rangle$ for case I (with $s_0 = 2.2$ and

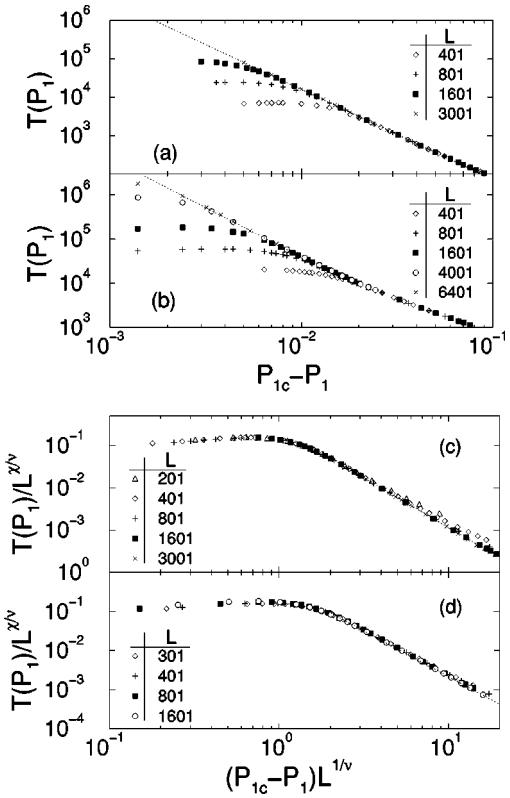

FIG. 4. Total strain as a function of P_1 and its scaling plots. (a) is for $s_0 = 2.2$ and (b) is for $s_0 = 10$ with $K_0 = 0$. A power-law fit yields (a) $-2.34(2)$ and (b) $-2.36(4)$. Dotted lines in (a) and (b) are power-law fits to the data. (c) and (d) are scaling plots for case I and II shown in Fig. 1: (c) and (d) are for $K_0 = 0$ and 0.01 with $s_0 = 2.2$, respectively. Here, $\chi/\nu = 1.79$ and $\nu = 4/3$ with the critical points P_{1c} given in Fig. 2.

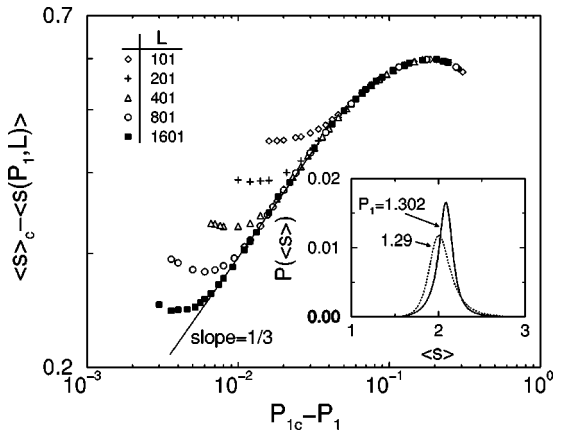

FIG. 5. The mean strain as a function of P_1 for the case shown in Fig. 1(a). The asymptotic mean strain at the critical point is $\langle s\rangle_c = 2.14$. The inset shows the distribution of the mean strain for $s_0 = 7$, $K_0 = 0$ and $L = 801$.

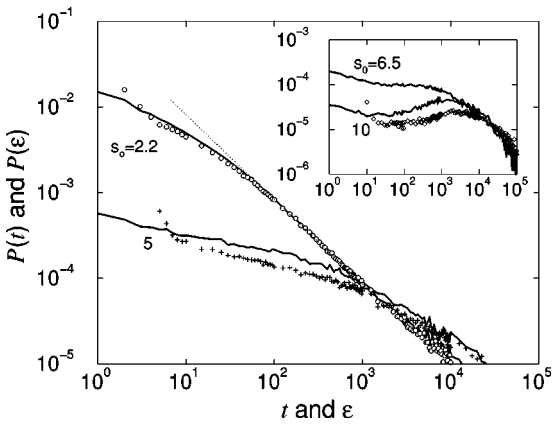

FIG. 6. Probability distribution of cluster size t and total strain ε, $\mathcal{P}(t)$ and $\mathcal{P}(\varepsilon)$, as a function of the initial strain $s_0 = 2.2, 5, 6.5$, and 10. Solid lines are for $\mathcal{P}(t)$ and symbols are for $\mathcal{P}(\varepsilon)$. For clarity, we plot $\mathcal{P}(\varepsilon)$ only for $s_0 = 2.2(\bigcirc)$, $5(+)$, and $10(\diamond)$. Here, $K_0 = 0$ and $P_1 = 1.2986$ with $L = 1599$ for $\mathcal{P}(t)$ and $L = 801$ for $\mathcal{P}(\varepsilon)$. The dotted line is a guide line with slope = -1.

10) as well as its scaling result for case I and II shown in Fig. 1. Near the critical point, the total strain T is well described by a power law such that $T(P_1) \sim (P_{1c} - P_1)^{-\chi}$ with $\chi = 2.35(2)$ as shown in Figs. 4(a) and 4(b). The deviation from the power law is due to finite-size effects. Note that the critical exponent for the total strain is $\chi \approx \gamma = 2.389$, where γ is the critical exponent for the mean cluster size $S(P_1) \sim (P_{1c} - P_1)^{-\gamma}$. As can be seen in Fig. 4(b), for a large initial strain of $s_0 = 10$, a much larger system size is required to see the asymptotic power-law behavior due to the effect of the initiation point. The excellent scaling collapse in Fig. 4(c) and 4(d) confirms that the total strain is simply proportional to the mean cluster size, and implies that for a large system size, the total strain has the same scaling law as the geometrical mean cluster size S,

$$T(P_1, L) \sim L^{\chi/\nu} \mathcal{Q}(L/\xi_g), \tag{3}$$

where $\chi = \gamma$ and $\nu = 4/3$. The scaling function in Eq. (3) is $\mathcal{Q}(x) \sim x^{-\chi/\nu}$ for $x \gg 1$ and $\mathcal{Q}(x) \sim$ const. for $x \ll 1$ with the geometrical correlation length $\xi_g(P_1) \sim |P_{1c} - P_1|^{-\nu}$. Thus, this result illustrates that the geometrical behavior dominates the strain behavior, and clearly demonstrates that the total strain displays universal behavior regardless of the value of K_0 and s_0.

Further insight into the dominant role of geometry on the strain variable can be obtained by examining the mean strain per strained site, $\langle s(P_1)\rangle = \langle \varepsilon(P_1)/t(P_1)\rangle$, where t and $\varepsilon = \Sigma_{\mathbf{r}} s(\mathbf{r}, P_1)$ are the cluster size and total strain for each simulation, respectively. It is clear from Fig. 5 that $\langle s\rangle_c - \langle s(P_1)\rangle$ also exhibits power-law behavior near the critical point, and the critical behavior of the mean strain can be described by

$$\langle s\rangle_c - \langle s(P_1)\rangle \sim |P_{1c} - P_1|^{\kappa}, \tag{4}$$

where $\langle s\rangle_c$ is the asymptotic mean strain at the critical point. The exponent is $\kappa = 0.33(1)$ and $0.91(2)$ for $K_0 = 0$ and 0.01, respectively, when $s_0 = 2.2$. Note that since $\kappa > 0$, when $P_1 \to P_{1c}, \langle s\rangle_c - \langle s(P_1)\rangle \to 0$, and this behavior is consistent with the asymptotic scaling result of $T(P_1)/S(P_1) = \langle \varepsilon(P_1)\rangle / \langle t(P_1)\rangle \sim$ const.

Since if $\varepsilon(P_1) \sim t(P_1)$, then $\kappa = 0$, Eq. (4) suggests that there might be a small correction to scaling for the total strain. Using $S(P_1) \sim |P_{1c} - P_1|^{-\gamma}$ with an approximation $\langle s(P_1)\rangle \approx \langle \varepsilon(P_1)\rangle / \langle t(P_1)\rangle$, one can estimate roughly the correction from $T(P_1) \approx |P_{1c} - P_1|^{-\gamma}(T_0 + T_{corr.})$ where $T_0 \approx a\langle s\rangle_c$ is constant (where a is also constant) and the correction term is $T_{corr.} \sim |P_{1c} - P_1|^{\kappa'}$ with $\kappa' = \kappa$; an actual calculation yields $\kappa' \approx 3/4$ and $T_0 \approx 2.2$ for $s_0 = 2.2$ and $K_0 = 0$. As the system approaches the critical point, however, the correction becomes negligibly small compared to the leading term T_0, and eventually, the asymptotic scaling form given in Eq. (3) is recovered. Thus, the exponent $\kappa(>0)$ implies the presence of a correction to scaling and determines the decay rate toward the asymptotic mean strain. Since we find that the value of κ depends strongly on the strain related model parameters s_0, P_2, and K_0, κ appears not to be a universal exponent. The inset of Fig. 5 shows the distribution of the mean strain, $\mathcal{P}(\langle s\rangle)$ for case I with $s_0 = 7$. As the system approaches the critical point, the location of the peak moves toward the critical value $\langle s\rangle_c$ and the distribution becomes sharper. We conclude that the geometry of a strained cluster is determined by the geometrical correlation length ξ_g, but a decay toward the asymptotic mean strain is controlled by the strain-dependent exponent κ.

Figure 6 shows the probability distributions for the cluster size and total strain, where for example, $\mathcal{P}(t)\,dt$ is the average number of clusters found to have size t. When the initial strain $s_0 = 2.2$, the size distribution $\mathcal{P}(t)$ exhibits a power-law decay, but as s_0 increases from $s_0 = 2.2$, the distribution seems to change from the power-law decay to a localized function. When $s_0 = 2.2$, we find that $\mathcal{P}(t)$ exhibits the same universal behavior as standard 2D percolation theory [11],

$$\mathcal{P}(t) \sim t^{-(\tau-1)} f(t/t'), \tag{5}$$

with $\tau=2.055$. $f(t/t')$ is a scaling function with the cutoff cluster size $t' \propto (P_{1c}-P_1)^{-1/\sigma'}$ and $\sigma'=36/91$ [11]. The scaling function in Eq. (5) is $f(x)\sim\exp[-x]$ for $x \gg 1$ and $f(x)\sim$const. for $x \ll 1$. Here, we neglect small t behavior, which results from the discreteness of the lattice.

When $s_0 \neq 2.2$, depending on the value of s_0, the exponent τ for the size distribution $\mathcal{P}(t)$ appears to deviate from its universal value. However, there is no distinctive region exhibiting a persistent power-law decay due to the curvatures, which may represent an initial strain-dependent long-transient behavior before crossing over to the true asymptotic, universal behavior. Note from Fig. 6 that the total strain probability distribution $\mathcal{P}(\varepsilon)$ also shows a similar behavior as that observed in $\mathcal{P}(t)$—a universal power-law distribution for $s_0=2.2$, as compared with a localized distribution for a large initial strain that also might be the same transient behavior. These results suggest that for $s_0>2.2$, the true asymptotic power-law decay with $\tau-1\approx 1$ probably emerges when $t>t_c$ and $\varepsilon>\varepsilon_c$, where t_c and ε_c are crossover values to the asymptotic regime, respectively, and are roughly t_c, $\varepsilon_c \approx 10^4$; for $s_0=2.2$, t_c, $\varepsilon_c \approx 10^2$. Thus, the small $t(<t_c)$ as well as ε $(<\varepsilon_c)$ behavior is possibly all transient. From Fig. 6 as well as Figs. 4(a) and 4(b), it is reasonable to assume that t_c and ε_c exhibit an initial-strain dependence since as s_0 increases, the scaling regime becomes narrower. When $s_0 \neq 2.2$, although we are unable to observe the true asymptotic behavior because of the huge values of t_c and ε_c, this argument seems to be consistent with the universal behavior found in the total strain and cluster size.

So far, we have considered the critical behavior of strain related quantities such as the total and mean strain, and their distributions for model *A* in the subcritical regime. Scaling analysis shows that the total strain exhibits critical power-law behavior with the universal exponent γ. This universal behavior results from the dominating role of the cells having the minimum stable strain. In the Sec. III B, we examine strain correlation functions for model *A* and explain the universal aspects of the model in terms of the strain correlation length.

B. Strain-strain correlation function and strain fluctuations

The geometrical density-density correlation function $C_g(\mathbf{r})$ is usually defined as $C_g(\mathbf{r})=\langle \rho(0)\rho(\mathbf{r})\rangle$, where $\rho(\mathbf{r})=1$ if a site $\mathbf{r}$ is occupied, otherwise $\rho(\mathbf{r})=0$ and $\mathbf{r}\neq 0$. It is known from standard percolation theory that the density correlation function decays as $C_g(r)\sim r^{-2\beta/\nu}\exp[-r/\xi_g]$ near a critical point with $\beta=5/36$ in 2D. In a similar way, we define the strain-strain correlation function $C_s(\mathbf{r})$ as

$$C_s(\mathbf{r})=\langle \hat{s}(0)\hat{s}(\mathbf{r})\rangle=\left\langle (1/N)\sum_{\mathbf{r}'}^{N} \hat{s}(\mathbf{r}')\hat{s}(\mathbf{r}+\mathbf{r}') \right\rangle_{\text{sims}}, \tag{6}$$

where $\hat{s}(\mathbf{r})=s(\mathbf{r})-\langle s\rangle$ with $\langle \hat{s}(\mathbf{r})\rangle=0$, N is the number of strained cells, and $\langle\rangle_{\text{sims}}$ denotes an average over many simulations. One may also consider a strain correlation function

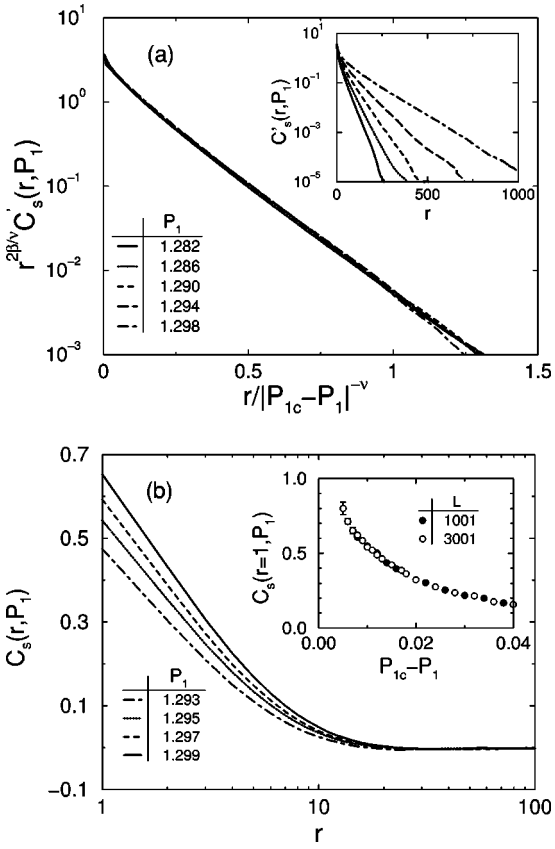

FIG. 7. Correlation functions for case I ($K_0=0$) with $s_0=2.2$ and $L=3001$. The inset of (a) shows $C_s'(r)$ and (a) is for scaling of $C_s'(r)$ with $\beta=5/36$ and $\nu=4/3$. (b) shows $C_s(r)$ and the inset shows $C_s(r,P_1)$ for $r=1$.

very similar to $C_g(\mathbf{r})$, that is, $C_s'(\mathbf{r})=\langle s(0)s(\mathbf{r})\rangle = \langle (1/N)\Sigma_{\mathbf{r}'}^{N} s(\mathbf{r}')s(\mathbf{r}+\mathbf{r}')\rangle_{\text{sims}}$. Note the difference between $C_s'(\mathbf{r})$ and $C_s(\mathbf{r})$, where the former one measures the strain correlation between two cells separated by $\mathbf{r}$, while the latter one measures the correlation of fluctuations from the mean strain. Due to the universal behavior found in the system, one can expect $C_s'(r)\sim r^{-2\beta/\nu}\exp[-r/\xi_g]$ with $\beta/\nu=5/48$. Indeed, we confirmed the universal scaling for $s_0=2.2$ and $K_0=0$; see Fig. 7(a). A simple mean field (MF) solution for the strain correlation function has been obtained as

$$C_s^{\text{MF}}(r)=(\mathcal{N}_s/2\alpha)\exp[-\alpha r], \tag{7}$$

where $\mathcal{N}_s$ is the noise strength and $\alpha=|(1-P_1)/P_1|$ [2]. Thus, the MF solution predicts a divergence at the mean field critical point $P_{1c}^{\text{MF}}=1$ and an exponential decay.

Figure 7(b) shows our simulation results for the model *A* correlation function $C_s(r)$ with $s_0=2.2$ and $K_0=0$. For small r, the correlation function appears to exhibit a fast logarithmic decay, and as shown in the inset of Fig. 7, $C_s(r,P_1)$ diverges at the critical point $P_{1c}=1.306$ when r is small. On the other hand, for a larger $r\simeq 10$, $C_s(r)$ exhibits an exponential decay and when $r\geqslant 30$, $C_s(r)\approx 0$. This fast decay to zero indicates that the strain correlation length ξ_s for the correlation function defined in Eq. (6) is small, and

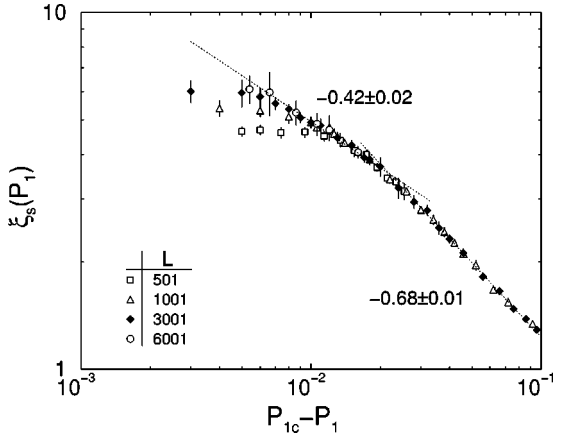

FIG. 8. The strain correlation length ξ_s as a function of P_1 for $s_0=2.2$ and $K_0=0$.

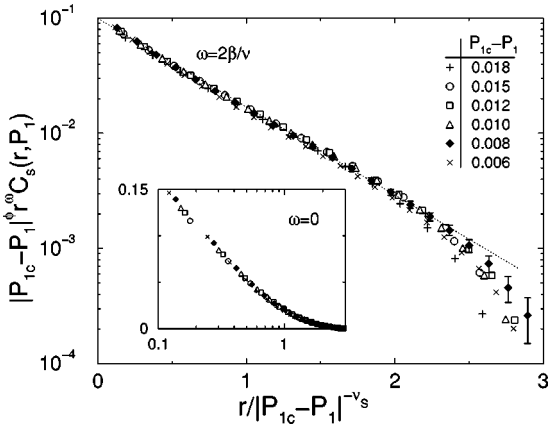

FIG. 9. Scaling of the correlation function $C_s(r)$ with $\nu_s=\phi=0.42$ and $\omega=2\beta/\nu=5/24$, where $1.288\leqslant P_1\leqslant 1.30$ and $P_{1c}=1.306$. The dotted line is a guide line indicating an exponential decay. The inset shows scaling with $\nu_s=0.42$, $\phi=0.31$, and $\omega=0$. Note that the inset is a log-linear plot. In both plots, $s_0=2.2$, $K_0=0$, and $L=3001$.

that any divergence at the critical point will be weak. Figure 8 shows the strain correlation length ξ_s defined as $\xi_s(P_1)^2=\Sigma_{\mathbf{r}} r^2 C_s(\mathbf{r},P_1)/\Sigma_{\mathbf{r}} C_s(\mathbf{r},P_1)$. These simulations suggest that the strain correlation length also exhibits a power-law behavior,

$$\xi_s(P_1)\sim|P_{1c}-P_1|^{-\nu_s}, \tag{8}$$

where the exponent $\nu_s=0.42$ for the critical region ($P_{1c}-P_1<0.02$) but ν_s deviates from the value when $P_{1c}-P_1>0.02$; also note that the deviation from the power law near the critical point is due to finite-size effects. Since the ratio $\nu_s/\nu\approx 0.32$, is smaller than unity, geometrical aspects of the model will dominate over strain aspects, and the total strain is thus well described by standard 2D percolation theory. Although we have calculated the correlation function for a different initial strain with a large system size to determine whether or not the exponent ν_s is independent of our model parameters used here, it is inconclusive because it requires a huge amount of computational time to observe at least one decade of power-law behavior near the critical point.

Figure 9 shows a successful scaling relation for $C_s(r)$,

$$C_s(r,P_1)\sim|P_{1c}-P_1|^{-\phi} r^{-\omega}\mathcal{F}(r/\xi_s) \tag{9}$$

with $\nu_s=\phi=0.42$ and $\omega=2\beta/\nu=5/24$, where the scaling function is $\mathcal{F}(x)\sim\exp[-x]$. In the inset, however, it is shown that with $\nu_s=0.42$, $\phi=0.31$, and $\omega=0$, an even better scaling is obtained with $C_s(r)\sim|P_{1c}-P_1|^{-\phi} g(r/\xi_s)$ where the scaling function $g(x)\sim-\ln(x)$ for small x and $\sim\exp[-x]$ for large x. Equation (9) is appealing because it has the universal power-law relation such as $C(r)\sim r^{-2\beta/\nu}$ for $r\ll\xi$ and ξ not too small. However, we are not able to examine the true small r regime because of the soft singularity at the critical point. That is, extremely large system sizes must be used to get sufficiently close to the critical point so that ξ_s can be adequately large. Therefore, we are not able to say that the correlation function C_s has the universal form, or whether some other scaling law pertains. Similarly, we cannot demonstrate theoretically any connection between the strain exponents and the geometric exponents. It is worth mentioning, however, that since any scaling attempt with $\nu_s=\nu$ or $\phi=0$ yields a systematic deviation, it might be reasonable to exclude such possibilities.

Equation (9) applies to an infinite system. For finite systems, the strain correlation length ξ_s at the critical point is limited by the system size L, and $|P_{1c}-P_1|^{-\phi}$ is also finite due to finite-size effects. Also note that the singularity of $\mathcal{F}$ at the origin is not seen because the lattice discreteness is important when $r\approx 1$. On the other hand, when $P_{1c}-P_1>0.03$, i.e., sufficiently far from the critical point, the strain correlation function behaves as $C_s(r=1,P_1)\sim(P_{1c}-P_1)^{-1}\exp[-c(P_{1c}-P_1)]$ with a constant c, which is not shown here to avoid overcrowding of figures. This result is in good agreement with the MF solution given in Eq. (7) except that $P_{1c}^{\mathrm{MF}}\neq P_{1c}$; we also observed the same behavior for $r=2$. Since the MF solution neglects fluctuations in the strain, $s(\mathbf{r})$, and the strained cluster size is quite small when P_1 is far from P_{1c}, a MF theory is valid for large $|P_{1c}-P_1|$.

C. Supercritical regime ($P_1>P_{1c}$)

In the thermodynamic limit, a cluster always spans the whole system when $P_1>P_{1c}$ but only a localized cluster exists when $P_1<P_{1c}$. For case I at the critical point, the total strain behaves as $T(P_{1c},L)\sim L^{d_f}$ with the fractal dimension $d_f=1.896(3)$, as shown in the inset of Fig. 10 and this holds also for the mean cluster size with the same d_f. For case II with the set of parameters shown in Fig. 1(b), we obtained $d_f=1.9(1)$, which is consistent with the case I result. It is known from standard percolation theory [11] that the critical exponents for the cluster size and correlation length, γ and ν, are connected to the fractal dimension d_f by the hyperscaling relation,

$$d_f=(1/2)(D+\gamma/\nu), \tag{10}$$

where D is the dimension of the system; in our case, $D=2$. Since the critical exponent for the total strain is $\chi=\gamma$, the

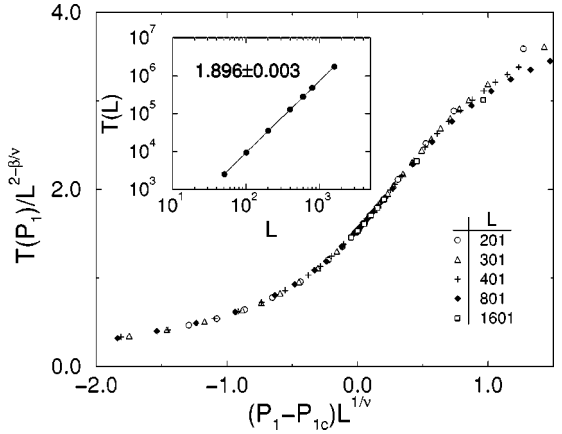

FIG. 10. Scaling of the total strain for $s_0=2.2$, $s_m=40$, $K_0=0$ (case I), and $P_{1c}=1.3062$. Here, $\beta=5/36$ and $\nu=4/3$. The inset shows the total strain at the critical point for the case shown in Fig. 1(a) as a function of the system size L, yielding the fractal dimension $d_f=1.896(3)$; for $s_m=40$, $d_f=1.895(6)$. Note that relaxation from $s_m=40$ does not affect the scaling.

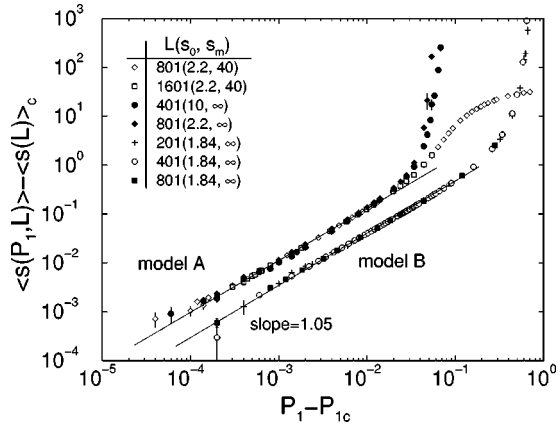

FIG. 11. Increase of the mean strain from its critical value for model *A* and *B* as a function of s_0 and s_m with $K_0=0$. Solid lines are guide lines with slope $=1.05(1)$.

fractal dimension of a strained cluster and its total strain for the cases shown in Fig. 1 can be calculated as $d_f=(1/2)(D+\chi/\nu)=1.8958$. Our results are in very good agreement with this prediction. This result implies the very important physical conclusion that in order to have a finite nonzero strain per site in the thermodynamic limit, the percolation control parameter P_1 should be $P_1>P_{1c}$ because $T(P_{1c},L)/L^2\sim L^{d_f-2}\to 0$ as $L\to\infty$. But of course, in a finite system, the strain is finite and nonzero at P_{1c}. Thus, for finite systems, the strain at the *critical point* must exhibit size dependence. As we will now show, there is a region above the critical point where the strain is well behaved.

Our finding of $T(P_{1c},L)\sim L^{d_f}$ implies that the strain per lattice site, $T(P_1,L)/L^2$, exhibits the same scaling behavior as $\mathcal{P}_{span}(P_1,L)$ does, where $\mathcal{P}_{span}(P_1,L)$ is the probability that a site belongs to a spanning cluster. As shown in Fig. 10, the strain per lattice site for case I is

$$T(P_1,L)/L^2\sim L^{-\beta/\nu}\mathcal{G}(L/\xi_g) \tag{11}$$

through the critical point, but with $|P_1-P_{1c}|$ small. The scaling function $\mathcal{G}(x)$ is constant for $x\ll 1$ and $\mathcal{G}(x)\sim x^{\beta/\nu}$ for $x\gg 1$. Thus, for an infinite size of system, the strain per lattice site is $T(P_1,L)/L^2\sim(P_1-P_{1c})^{\beta}$, that is, $T(P_1,L)/L^2$ is well behaved at P_{1c}, not singular. So far, we have considered model *A*. Not surprisingly, the total strain of model *B* also exhibits the same universal behavior as observed in model *A*, but with a slightly different critical point $P_{1c}=1.340(2)$ for $s_0=1.84$ and $K_0=0$.

These results for the total strain in the vicinity of the critical point also imply that the mean strain, $\langle s(P_1,L)\rangle-\langle s(L)\rangle_c$ is likewise nonsingular there. This is shown for case I in Fig. 11, where $\langle s(P_1,L)\rangle-\langle s(L)\rangle_c\sim(P_1-P_{1c})^{\kappa}$ with $\kappa=1.05(1)$ is found near the critical point. Both model *A* and *B* display the same power-law increase. This result implies that in the thermodynamic limit, $\langle s(P_1)\rangle-\langle s\rangle_c\sim(P_1-P_{1c})^{\kappa}$. For model *A*, approximately when $P_1>P_{1c}+0.02$, the mean strain per strained site, $\langle s(P_1)\rangle$, begins to deviate from the power law and diverges exponentially if $s_m=\infty$ or converges to a finite asymptotic value, s_m, if $s_m\neq\infty$. As can be seen in Fig. 11, this avalanche point (where the mean strain diverges) changes depending on the type of strain propagation—model *A* or *B*—and probably on the density of locks, but seemingly not on the initial strain.

The almost linear increase in the mean strain near P_{1c} can be explained by noting that in this regime, the shape of a spanning cluster is no longer fractal but rather compact with a continuous increase in the total strain and the mean cluster size. Therefore, by taking a Taylor expansion of $\langle s(P_1)\rangle$, we obtained a linear increase, i.e.,

$$\langle s(P_1)\rangle-\langle s\rangle_c\approx\frac{\partial\langle s(P_1)\rangle}{\partial P_1}\Big|_{P_{1c}}(P_1-P_{1c}). \tag{12}$$

The Taylor expansion is valid, of course, only if the mean strain is well behaved at the critical point.

When $K\neq 0$, these results no longer hold, probably because the activation of the second mechanism in some cells increases the mean strain rather abruptly with increasing probability K in Eq. (1). For case II with the set of parameters shown in Fig. 1(b), we observed a deviation from the linear increase with $\kappa=1.3(1)$ that is not shown here. However, the finite separation between the critical point and the avalanche point still holds.

We close this section with the observation that since a large deforming system demands a finite strain from a percolation event, this can only be accomplished by the physical system inhabiting the region between the critical and avalanche points. So this narrow region is very important, physically.

IV. CONCLUSIONS

Our simple strain percolation model, which captures the essential mechanisms of strain propagation through dislocation cell walls, suggests that a deforming metal is a self-organizing system with universal scaling properties. A stochastic linear response of dislocations in one cell wall to

other dislocations generated in a neighboring cell with an occasional breaking of unstable dislocation locks in the wall is our key physical picture for the strain transmission from one cell to another. The criticality of our model is characterized by critical exponents and a few model parameters. The model parameters control the wall response as described above, and are assumed to be functions of the macroscopic stress and strain. As the percolation model parameters increase, the overall system progresses from a subcritical regime of essentially negligible macroscopic strain to a critical state above which the strain is nonzero in the thermodynamic limit, and finally to strain avalanche. Between the critical point and the avalanche point, lies a narrow region of stable total system strain growth.

The fractal geometry of a strained cluster at the critical point implies that the macroscopic strain there is zero for systems where size effects can be neglected, and finite strain is observed only in the supercritical regime. Nevertheless, the critical point separates the region of finite strain from zero strain, and can serve as a physical definition of the flow stress for the system.

As the system approaches the critical point, the majority of the strained cells in a strained cluster take on a strain value that is independent of the initiating strain. This strain value is that, which is marginally capable of being propagated indefinitely through the system, and is only slightly larger than the strain below which an initiating strain cannot propagate at all. We have shown that the existence of this critical value for the mean strain follows directly from the discrete nature of the dislocations, and amounts to a kind of ''organization'' of the strain near its minimum transmission value. The existence of a finite nonzero mean strain at the critical point is the reason why the strain per strained site is well behaved through the critical point and also why the critical point is separated slightly from the avalanche point. (In mean field, the critical and avalanche points are synonymous.)

One of our central findings is that near the critical point, the total strain exhibits critical power-law behavior with universal critical exponents, which are related to standard 2D percolation theory. This connection to standard percolation theory exists even though the standard theory contains no variable corresponding to the strain variable of our model. It turns out that in the critical regime, the strain correlation length is much smaller than the geometrical correlation length. Consequently, the critical behavior of the physical quantities associated with the strain variable are dominated by the geometrical aspects of the model, which we have shown are in the same universality class as standard percolation theory. In other words, the universal behavior of the total strain in the system is a consequence of the self-organizing character of the strain in the critical cluster described in the preceding paragraph.

Due to the narrow scaling regime, the precise form of a scaling function for the strain fluctuation correlation function (C_s) has not been found. However, we surmise that a weak power-law decay with an universal exponent might be characteristic of the correlation function near the critical point because of the universal behavior of the model, which we presume is related to the self-organizing strain behavior. On the other hand, the strain correlation function (C_s') is well described by a universal scaling function. We also showed that the mean field theory for the strain correlation function (which shows an exponential decay with distance), is valid when the system is subcritical and not too near the critical point.

In this paper, although we have reported results for one set of case II parameters, we have focused mainly on case I (with no lock unzipping). We will report more systematically on case II in a subsequent paper. Also, we hope to explore the effect of cell size variation in a later investigation.

Finally, we note that the detailed connection between our model and actual metal deformation has not been made in this paper. Suffice it here to say simply that the percolation model is intended to correspond to the fine slip which appears at all stages of deformation. The complex connection between the fine slip and the total deformation in the system is left to subsequent papers.

ACKNOWLEDGMENT

R. Thomson gratefully acknowledges partial support from Pacific Northwest National Laboratory.

[1] R. Thomson and L. E. Levine, Phys. Rev. Lett. **81**, 3884 (1998).
[2] R. Thomson, L. E. Levine, and D. Stauffer, Physica A **283**, 307 (2000).
[3] L. P. Kubin, in *Materials Science and Technology: A Comprehensive Treatment*, edited by R. W. Cahn, P. Haasen, and E. J. Kramer (VCH, Weinheim, 1993), Vol. 6, p. 137.
[4] J. Gil Sevillano, in *Materials Science and Technology: A Comprehensive Treatment* (Ref. [3]), Vol. 6, p. 19.
[5] S. Mader, Z. Phys. **149**, 73 (1957).
[6] A. Seeger, in *Dislocations and Mechanical Properties of Crystals*, edited by J. Fisher *et al.* (Wiley, New York, 1956).
[7] T. Noggle and J. Koehler, J. Appl. Phys. **28**, 53 (1957).
[8] D. E. Kramer (unpublished).
[9] R. B. Pond, Sr., in *The Inhomogeneity of Plastic Deformation* (American Society for Metals, Metals Park, OH, 1973), p. 1.
[10] H. Neuhauser, in *Dislocations in Solids*, edited by F. R. N. Nabarro (North-Holland, Amsterdam, 1983), Vol. 6.
[11] D. Stauffer and A. Aharony, *Introduction to Percolation Theory* (Taylor & Francis, London, 1994).
[12] B. K. Chakrabarti and L. G. Benguigui, *Statistical Physics of Fracture and Breakdown in Disordered Systems* (Oxford University Press, New York, 1997).
[13] M. Sahimi, *Flow and Transport in Porous Media and Fractured Rock* (VCH, Weinheim, New York, 1995).
[14] P. Bak, C. Tang, and K. Wiesenfeld, Phys. Rev. Lett. **59**, 381 (1987).
[15] Z. Olami, Hans Jacob S. Feder, and K. Christensen, Phys. Rev. Lett. **68**, 1244 (1992).

[16] S. Clar, B. Drossel, and F. Schwabl, Phys. Rev. Lett. **75**, 2722 (1995); B. Drossel, *ibid.* **76**, 936 (1996).
[17] H. J. Jensen, *Self-Organized Criticality* (Cambridge University Press, Cambridge, 1998).
[18] H. Mughrabi, T. Ungar, W. Kienle, and M. Wilkens, Philos. Mag. A **53**, 793 (1986).
[19] I. Groma and B. Bako, Phys. Rev. Lett. **84**, 1487 (2000).
[20] P. Hähner, K. Bay, and M. Zaiser, Phys. Rev. Lett. **81**, 2470 (1998).
[21] U. F. Kocks, in *Dislocations and Properties of Real Materials* (Institute of Metals, London, 1985).
[22] F. J. Jimenez, Master thesis, Faculty of Engineering, University of Navarra, San Sebastián, Spain, 1982; see also Refs. [3,4].
[23] M. Kardar, Phys. Rep. **301**, 85 (1998).
[24] D. Hull and D. J. Bacon, *Introduction to Dislocations* (Butterworth-Heinemann, Woburn, 1999), p. 207.
[25] P. L. Leath, Phys. Rev. B **14**, 5046 (1976).